Therefore, both transverse and longitudinal feedback systems are required to damp the multi-bunch instabilities. The electron cloud density is calculated with different SEY and bunch spacing. A SEY lower than 1.6 and bunch spacing longer than 25 ns are suggested to eliminate the electron cloud instability.

2.7.7 References

1. E. Keil and W. Schnell, CERN Report, TH-RF/69-48 (1969).
2. D. Boussard, CERN LAB II/RF/Int./75-2 (1975).
3. A. Chao, "Physics of collective beam instabilities in high energy accelerators", John Wiley & Sons, Inc. (1993).
4. S. Krinsky, et al., "Collective effects in the NSLS-II storage ring", Proceedings of PAC07, TUPMS074 (2007).
5. ABCI Home Page, http://abci.kek.jp/abci.htm
6. www.cst.com
7. M. Borland, "elegant: A Flexible SDDS-Compliant Code for Accelerator Simulation", Advanced Photon Source LS-287 (2000).
8. Y. Wang and M. Borland, "Pelegant: A Parallel Accelerator Simulation Code for Electron Generation and Tracking", Proceedings of the 12th Advanced Accelerator Concepts Workshop, AIP Conf. Proc. 877, 241 (2006).
9. F. Zimmermann, G. Rumolo, "Two-stream Problems in Accelerators", CERN SL-2001-057(AP) (2001).
10. E. Benedetto, D. Schulte and F. Zimmermann, "Simulation study of electron cloud induced instabilities and emittance growth for the CERN Large Hadron Collider proton beam", Phys. Rev. ST Accel. Beams 8, 124402 (2005).
11. Y. Bacconier and G. Brianti, "The stability of ions in bunched beam machines", CERN/SPS/80-2 (1980).
12. L. Wang, Y. Cai and T.O. Raubenheimer, "Suppression of beam-ion instability in electron rings with multibunch train beam fillings", Phys. Rev. ST Accel. Beams 14, 084401 (2011).

2.8 Some critical collective effects for the FCC-ee collider

Eleonora Belli[1,2], Giovanni Castorina[2], Mauro Migliorati[2], Serena Persichelli[4], G. Rumolo[1], Bruno Spataro[3], Mikhail Zobov[3]

[1]CERN, Geneva, Switzerland

[2]University of Rome 'La Sapienza' and INFN Sez. Roma1, Rome, Italy

[3]INFN/LNF, Frascati, Rome

[4]LBNL, Berkeley, California

Mail to: eleonora.belli@cern.ch

2.8.1 Introduction

In the framework of the Future Circular Collider (FCC) design studies at CERN [1], the high luminosity electron-positron collider FCC-ee is considered as a possible first step towards FCC-hh, a 100 TeV hadron collider in the same tunnel of about 100 km. Table 1 summarizes the main beam parameters at four different center-of-mass energies from

45.6 GeV (Z pole) to 175 GeV (top pair threshold). One of the major issues for such a kind of machine is represented by collective effects due to electromagnetic fields generated by the interaction of the beam with the vacuum chamber, which could produce instabilities, thus limiting the machine operation and performance. An impedance model is needed to study these instabilities, to predict their effects on the beam dynamics and to find a possible solution for their mitigation. Another critical aspect for the future lepton collider is represented by the electron cloud which will be discussed in the last section of this contribution, together with possible strategies to suppress its effects.

Table 1: FCC-ee baseline beam parameters [2].

Energy E_0 [GeV]	***45.6***	***80***	***120***	***175***
Circumference C [km]	97.75			
Bunch population N_p [10^{11}]	1.7	1.5	1.5	2.7
Number of bunches/beam	16640	2000	393	48
Beam current [mA]	1390	147	29	6.4
Momentum compaction α_c [10^{-5}]	1.48	0.73	0.73	0.73
Bunch length $\sigma_{z,SR}/\sigma_{z,BS}$ [mm]	3.5/12.1	3.3/7.65	3.15/4.9	2.45/3.25
Energy spread $\sigma_{dp,SR}/\sigma_{dp,BS}$ [%]	0.038/0.132	0.066/0.153	0.099/0.151	0.147/0.192
Horizontal tune Q_x	269.138	389.154	389.129	389.104
Vertical tune Q_y	269.22	391.22	391.199	391.176
Synchrotron tune Q_s	0.0248	0.0229	0.0357	0.0672
Horizontal emittance ε_x [nm]	0.27	0.28	0.63	1.34
Vertical emittance ε_y [pm]	1.0	1.0	2.3	2.7
SR energy loss per turn [GeV]	0.036	0.34	1.72	7.8
RF voltage [GV]	0.1	0.44	2.0	9.5

2.8.2 **Wake fields and impedances**

Collective beam instabilities induced by wake fields represent an active subject in the design of a particle accelerator and the theory behind this topic has been elaborated and refined over many years by several authors [3,4,5,6]. This section will describe the contributions of specific machine components to the total impedance budget and discuss their effects on the beam stability. Single bunch instability thresholds due to the resistive wall (RW) impedance will be estimated in both transverse and longitudinal planes and a longitudinal impedance budget including the contributions of several vacuum chamber components will be provided for the lowest energy case (Z pole at 45.6 GeV).

2.8.2.1 ***Resistive wall impedance and effects on beam dynamics***

When the beam passes through a vacuum chamber which is not perfectly conducting but characterized by a finite resistivity, it generates wake fields that can act on the following particles and perturb their motion, giving rise to instabilities that can occur in both the longitudinal and transverse planes. For a circular beam pipe with radius b and a single layer of infinite thickness, the longitudinal and transverse impedances per unit length are given, respectively, by [7,8,9]

$$\frac{Z_{\parallel}(\omega)}{C} = \frac{Z_0 c}{\pi} \frac{1}{[1 + i\mathrm{sgn}(\omega)]2bc\sqrt{\frac{Z_0 c \sigma_c}{2|\omega|}} - ib^2\omega} \quad (1)$$

and

$$\frac{Z_{\perp}(\omega)}{C} = \frac{Z_0 c^2}{\pi} \frac{1}{[\mathrm{sgn}(\omega)+i]b^3 c\sqrt{2\sigma_c Z_0 c|\omega|} - ib^4\omega^2} \quad (2)$$

where C is the machine circumference, Z_0 the vacuum impedance, c the speed of light and σ_c the material conductivity. In the case of FCC-ee, the value of the RW impedance produced by the finite conductivity of the copper chamber is increased by thin films of non-evaporable getter (NEG) materials. This coating is required to mitigate the electron cloud build up in the machine and to improve the pumping system [10,11], being characterized by a low Secondary Electron Yield (SEY), a low desorption yield and a very high pumping speed. The effect of the NEG coatings renders the contribution of the RW to the impedance budget critical for the machine design. It has been observed [12] that the thickness of the coating plays a fundamental role: The RW impedance decreases for a thinner coating and this results in higher single bunch instability thresholds, thus improving the beam stability during machine operation.

When computing the RW impedances with the ImpedanceWake2D code [13] (see Figure 1), the vacuum chamber is assumed to be circular with 35 mm radius and three layers (a first layer of copper with 2 mm thickness, then 6 mm of dielectric and finally iron with resistivity $\rho = 10^{-7}\Omega\mathrm{m}$), coated with NEG films of three different thicknesses ($1\ \mu\mathrm{m}, 250$ nm and 100 nm).

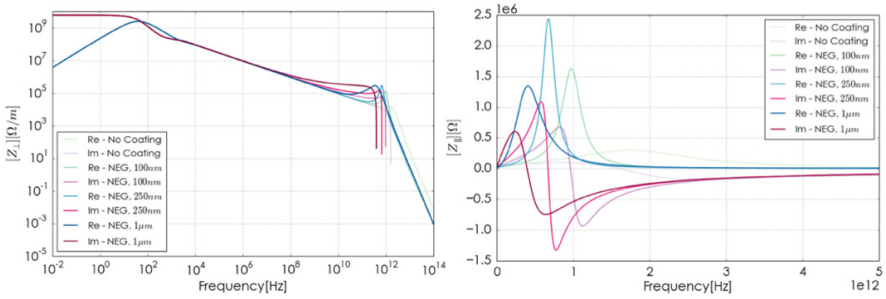

Figure 1: Real and imaginary part of the transverse (left) and longitudinal (right) RW impedances as a function of the frequency in the case of no coating and NEG coating with different thicknesses.

The following sections are focused on the most important effects of the RW on the single bunch dynamics: the Microwave Instability (MI) and the Transverse Mode Coupling Instability (TMCI) in the longitudinal and transverse planes, respectively. The main parameters used for the simulations are listed in Table 1.

2.8.2.1.1 Microwave instability

One consequence of the longitudinal microwave instability is the bunch lengthening, together with changes in the energy spread, which starts to increase above the instability

threshold. The bunch length and the energy spread as a function of the bunch intensity obtained from the macroparticle tracking code PyHEADTAIL [14] are shown in Figure 2, for all the cases under study. It is clearly visible that NEG film coatings must be thin(ner) to ensure the beam stability. In fact, in the case of 100 nm thickness the MI threshold is about two times larger than the nominal bunch intensity, while for a thicker coating of 1 μm the bunch is unstable. It is important to note that these studies do not take into account the beamstrahlung with colliding beams, which gives a much longer bunch and a higher energy spread, thus helping to increase the MI threshold.

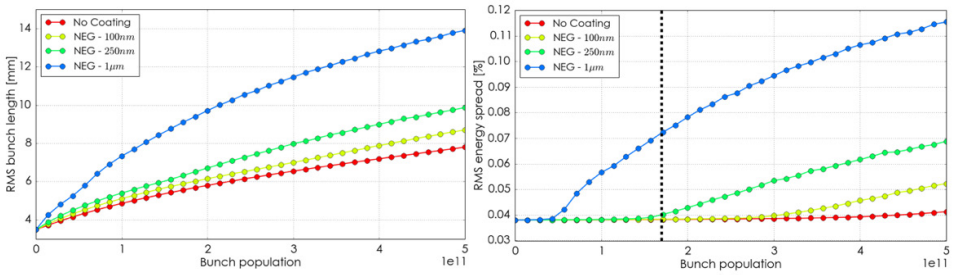

Figure 2: Bunch length and energy spread as a function of the bunch intensity by considering only the RW contribution for different thicknesses of the NEG films. The dashed black line represents the nominal bunch intensity.

2.8.2.1.2 Transverse mode coupling instability

It is well known from theory [4] that the betatron frequencies of the intra-bunch modes shift when the bunch intensity increases and the instability occurs when the mode frequency lines merge. Unlike the longitudinal case, above the instability threshold the bunch is lost in the transverse case and this makes the TMCI very dangerous for the beam.

Figure 3 shows the real part of the tune shift of the first two radial modes (with azimuthal number from -2 to 2) as a function of the bunch population for the case of 100 nm coating. The eigenfrequencies of the coherent modes (azimuthal and radial) in the transverse plane are computed with the analytical Vlasov solver DELPHI [15] by taking into account the bunch lengthening due to the longitudinal wake (yellow curve in Figure 2).

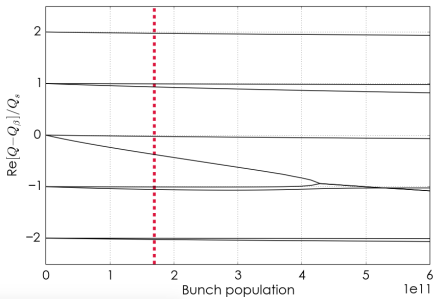

Figure 3: TMCI threshold, evaluated by considering only the RW contribution in the case of 100 nm thick NEG coating, and taking into account the bunch lengthening due to the longitudinal wake. The dashed red line represents the nominal bunch intensity.

2.8.2.2 *Other impedance sources*

Besides the RW, there are other important impedance sources in the machine to be analysed with particular care (see Figure 4). First of all, for Z running, the RF system consists of about fifty-six single-cell 400 MHz cavities, which will be arranged in groups of 4 cavities, connected by tapers. In addition, 10000 absorbers will be needed to cope with the synchrotron radiation (SR), which is an important source of heat and photoelectrons for high-energy lepton machines. In order to reduce the impedance contribution of the photon absorbers, it was decided to use a circular vacuum chamber with 35 mm radius and two rectangular antechambers on both sides, inside which the SR absorbers can be installed, as is the case for the SuperKEKB beam pipe [16]. Diagnostic elements like four-button beam position monitors (BPMs) [17] are also planned to be installed for a total number of about 4000, with a rotation angle of 45° in order to place them directly on the winglet chamber and to avoid special winglet-to-circular tapers whose contribution has been observed to be not negligible compared to the RW one [18]. Finally, a total number of 20 collimators [19] (10 for each plane) are considered in this model.

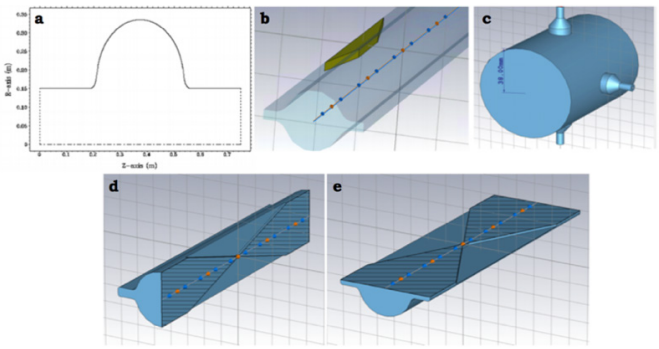

Figure 4: ABCI and CST models for a) RF cavities, b) SR absorbers, c) BPMs, d) vertical collimators and e) horizontal collimators.

In order to evaluate the contribution of all these components to the longitudinal impedance budget, CST [20] simulations in time domain were performed by considering a Gaussian bunch at the nominal bunch length of $\sigma_z = 3.5\,mm$. Figure 5 shows the comparison of the longitudinal wake potentials of each component with the RW one, obtained analytically as the convolution between the wake function computed by ImpedanceWake2D in the case of no coating and a 3.5 mm Gaussian bunch.
Figure 5 also contains an estimate of the loss factors for each component, corresponding to a total dissipated power of about 24.6 MW at the nominal intensity, about a factor 4 smaller than the total SR power dissipated by the two beams of about 100 MW. However, this value of power loss has to be considered as a conservative one and it is expected to be lower due to the bunch lengthening effect.

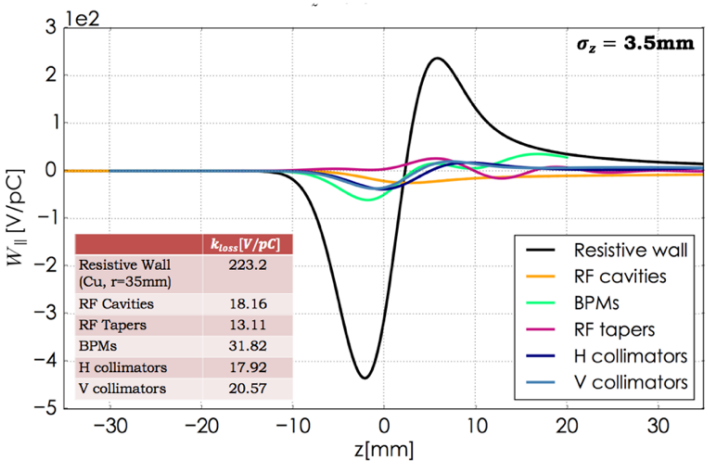

Figure 5: Total wake potentials for the nominal bunch length $\sigma_z = 3.5mm$ due to the several vacuum chamber components compared with the RW contribution (black line).

2.8.3 **Electron cloud**

Electron cloud (EC) effects represent one of the main performance limitations for both hadron and lepton machines [21, 22]. In the case of the lepton collider FCC-ee, primary electrons are attracted and accelerated by the positron beam and the electron accumulation in the vacuum chamber can cause the heating of the pipe walls and instabilities, beam losses, emittance growth and vacuum and diagnostics degradation. This section presents recent EC studies for FCC-ee. The EC build up will be analyzed in the arc dipoles of the machine and the use of EC maps will allow finding optimal filling schemes to reduce the heat load. An analytical estimation of the fast head-tail instability threshold will be given for all beam energies.

2.8.3.1 ***Electron cloud maps for FCC-ee dipoles***

The numerical simulations have been performed with the PyECLOUD code [23]. Primary electrons in the vacuum chamber are assumed to be generated by photoemission due to SR. In the case of FCC-ee at 45.6 GeV, the number of photoelectrons per particle per meter is given by $N_{ph} = N_\gamma Y$ where $N_y = \frac{5\alpha}{2\sqrt{3}}\frac{\gamma}{\rho} = 0.085$ is the number of photons per particle per meter and $Y = 0.04$ is the photoelectron yield, i.e. the probability of electron emission per impinging photon. A reflectivity of $R = 80\%$ is assumed in our simulations (in the presence of antechambers and photon stops, this assumption may be quite pessimistic), meaning that 80% of photoelectrons are generated by photons which are reflected from the chamber. Simulations were performed for FCC-ee dipoles with magnetic field $B = 0.014\,T$, at the nominal bunch population of 1.7x10^{11} and a bunch spacing of 2.5 ns, by scanning the SEY from 1.0 to 2.0.
Figure 6 shows the total number of electrons in the FCC-ee dipole chamber, assumed to be circular with radius $r = 35\text{mm}$, during the passage of a train of 1000 successive positron bunches followed by 400 empty bunches and for $\delta_{max} = 1.2$.

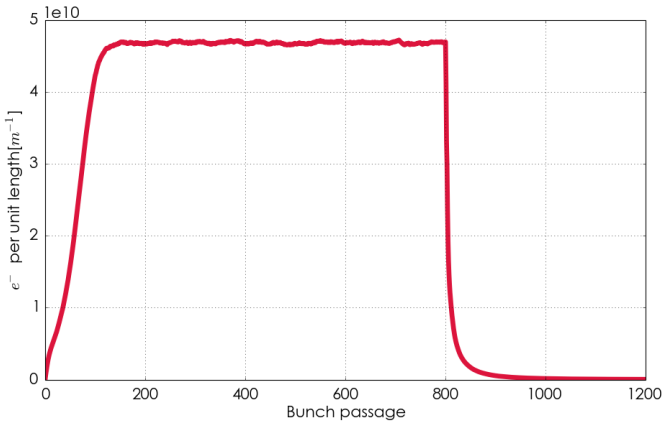

Figure 6: Time evolution of the total number of electrons in the chamber of the FCC-ee arc dipoles, for $Y = 0.04$, $R = 80\%$ and $\delta_{max} = 1.2$.

The electron density grows exponentially until a saturation level due to the space charge in the cloud of electrons and then it decays after the passage of the train. The rise time of the build up process and the decay time corresponding to the passage of the empty bunches can be expressed by means of a cubic map [24]

$$\rho_{m+1} = a\rho_m + b\rho_m^2 + c\rho_m^3 \tag{3}$$

whose coefficients depend only on the chamber (SEY, dimensions, etc.) and the beam parameters. Once these coefficients are extrapolated from a detailed build up simulation with a long train of bunches, they can be used to evaluate the electron density and the heat load evolution for different filling patterns. One possible application of the map formalism is the study of optimal filling schemes to reduce the build up process in the machine, with the advantage of a significant reduction of the simulation time.
Figure 7 shows the time evolution of the electron density and the heat load as a function of the SEY in the FCC-ee dipoles for three different filling schemes:

1. a long uniform train of 16640 bunches
2. 140 trains of 120 successive bunches followed by 200 empty bunches
3. 550 trains of 30 successive bunches followed by 100 empty bunches
    1.

The insertion of additional gaps in the bunch train allow to reduce the EC induced heat load by a factor of about 10. For comparison, the local heat load from synchrotron radiation is about 800 W/m.

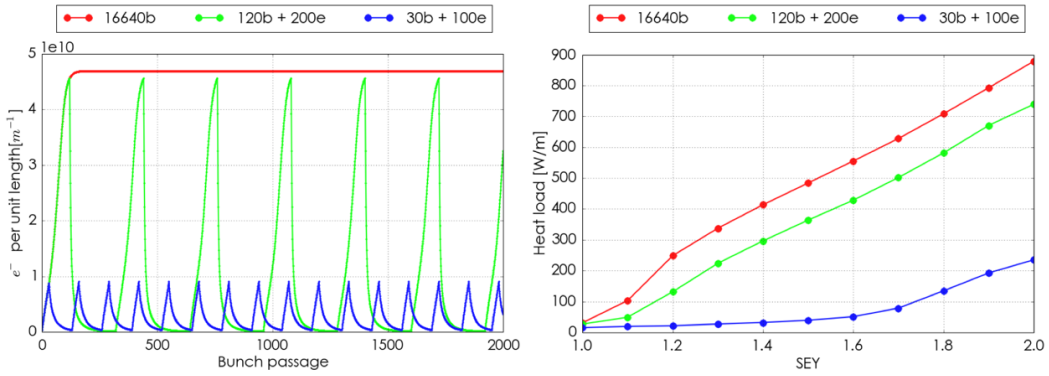

Figure 7: Electron density evolution (on the left) and heat load as a function of the SEY (on the right) in the FCC-ee arc dipoles for three different filling patterns, at nominal intensity $N = 1.7 \cdot 10^{11}$ and for $\delta_{max} = 1.2$.

2.8.3.2 *Electron density threshold for the single bunch head-tail instability*

EC single bunch head tail instability has been analysed and observed in several machines [25, 26]. This instability depends on the electron density near the beam whose threshold is given by

$$\rho_{th} = \frac{2\gamma Q_s}{\sqrt{3} Q r_e \beta C} \tag{3}$$

where r_e is the classical electron radius, $\beta_{x,y} = \frac{C}{2\pi Q_{x,y}}$ is the average beta of the machine and $Q = \min\left(\frac{\omega_e \sigma_z}{c}, 7\right)$ with ω_e the frequency of the electron oscillation near the beam centre [27]. Table 2 summarizes the electron density thresholds for FCC-ee at four energies, considering the baseline beam parameters shown in Table 1. Such low thresholds can create potential problems for the collider operation and this issue certainly deserves further investigations.

Table 2: Density thresholds of the fast head-tail instability for FCC-ee.

Energy E_0 [GeV]	**45.6**	**80**	**120**	**175**
Electron frequency $\frac{\omega_e}{2\pi}$ [GHz]	393.25	454.136	308.08	375.58
Electron oscillation $\frac{\omega_e \sigma_z}{c}$	28.847	31.41	20.34	19.28
Electron density threshold $\rho_{th}[10^{10}/m^3]$	**2.29**	**5.39**	**12.6**	**34.6**

2.8.4 References

1. https://fcc.web.cern.ch
2. D. Shatilov, "Luminosity optimization for FCC-ee: recent results", 59th FCC-ee Optics Design meeting, 25 Aug 2017, CERN, Geneva, Switzerland.
3. L. Palumbo, V.G. Vaccaro, M. Zobov, "Wake fields and impedances", Report No. LNF-94-041-P, 1994 and arXiv preprint physics/0309023 (2003).
4. A.W. Chao, "Physics of collective beam instabilities in high energy accelerators",

Wiley, 1993.
5. B. Zotter, S. Kheifets, “Impedances and Wakes in High Energy Particle Accelerators”, World Scientific, 1998.
6. K.Y. Ng, “Physics of intensity dependent beam instabilities”, World Scientific, 2006.
7. K.Y. Ng and K. Bane, “Explicit Expressions of Impedances and Wake Functions”, SLAC-PUB-15078, 2010.
8. E. Belli, M. Migliorati, S. Persichelli and M. Zobov, "Single beam collective effects in FCC-ee due to beam coupling impedance", arXiv preprint arXiv:1609.03495, 2016.
9. M. Migliorati et al., “Collective effects issues for FCC-ee”, eeFACT-2016-TUT3AH1.
10. https://kt.cern/technologies/non-evaporable-getter-neg-thin-film-coatings
11. A. Rossi, “SEY and electron cloud build-up with NEG materials”, 2005, CERN, Geneva, Switzerland.
12. E. Belli, “Impedance model and collective effects for FCC-ee”, FCC Week 2017, 29 May- 2 Jun 2017, Berlin, Germany.
13. https://twiki.cern.ch/twiki/bin/view/ABPComputing/ImpedanceWake2D
14. https://github.com/PyCOMPLETE/PyHEADTAIL
15. https://twiki.cern.ch/twiki/bin/view/ABPComputing/DELPHI
16. Y. Suetsugu, K. Kanazawa, K. Shibata, T. Ishibashi, H. Hisamatsu et al., “Design and construction of the SuperKEKB vacuum system”, Journal of Vacuum Science & Technology A: Vacuum, Surfaces, and Films 30.3 (2012): 031602.
17. A. R. D. Rodrigues et al. "Sirius status report." 7th International Particle Accelerator Conference (IPAC’16), Busan, Korea, May 8-13, 2016.
18. E. Belli et al., “Coupling impedances and collective effects for FCC-ee”, IPAC-2017-THPAB020.
19. T. Ishibashi et al., “Low impedance movable collimators for SuperKEKB”, Proceedings of IPAC’17, Copenhagen, Denmark, May 14-19, 2017.
20. https://www.cst.com
21. H. Fukuma, “Electron cloud instability in KEKB and SuperKEKB”, ICFA BDNL 48, p.112, Apr.2009.
22. G. Iadarola, “Electron cloud studies for CERN particle accelerators and simulation code development”, 2014.
23. https://github.com/PyCOMPLETE/PyECLOUD
24. U. Iriso, S. Peggs, “Maps for electron clouds”, Physical Review Special Topics-Accelerators and Beams 8.2 (2005): 024403.
25. G. Rumolo and F. Zimmermann, "Theory and Simulation of the Electron cloud instability." Proceedings of the LHC Workshop Chamonix XI. 2001.
26. K. Ohmi, F. Zimmermann, “Head-Tail Instability Caused by Electron Clouds in Positron Storage Rings”, PRL 85(18), pg.3821-3824 (2000).
27. K. Ohmi, F. Zimmermann and E. Perevedentsev, “Study of the fast head-tail instability caused by the electron cloud”, CERN-SL-2001-011 AP.